
Article:
Yan, Shuaicheng, Li, Donggen, Jiang, Weiheng et al. (2026) EE-SE Trade-Off in Deep Learning-Based URLLC Cell-Free Massive MIMO Systems. IEEE wireless communications letters. pp. 2388-2392. ISSN: 2162-2337

https://doi.org/10.1109/LWC.2026.3678625

EE-SE Trade-off in Deep Learning Based URLLC Cell-Free Massive MIMO Systems

Shuaicheng Yan, Donggen Li, Weiheng Jiang, Wenjiang Feng, Pei Xiao, *Senior Member, IEEE*, Kanapathippillai Cumanan, *Senior Member, IEEE*, Alister Burr, *Senior Member, IEEE*

***Abstract*—In smart Internet of Things (IoT) factories with dense terminal access, the communication scenarios and requirements differ significantly between ground terminals (GTs) and aerial terminals (ATs). Consequently, their demands for the two key performance indicators under URLLC constraints—Energy Efficiency (EE) and Spectral Efficiency (SE)—also exhibit distinct characteristics and variations. To achieve differentiated trade-offs between EE and SE for these two types of terminals, this letter proposes an unsupervised power allocation network (U-ESTPANet) and designs a differentiated trade-off mechanism. Compared with traditional iterative algorithms, it exhibits superior real-time performance and adaptability to complex scenarios. In contrast to fully supervised deep neural networks, this network can enhance the stability and real-time performance of outputs without the need for labeled training samples. Simulation results demonstrate that the proposed unsupervised method can effectively optimize the spectral efficiency and energy efficiency of the system.**

***Index Terms*—Smart IoT factory, energy efficiency, spectral efficiency, unsupervised learning, differentiated trade-off.**

I. Introduction

By leveraging the architectural advantages of distributed access points (APs), the cell-free massive MIMO (CF-mMIMO) system provides a solid foundation for large-scale dense terminals in smart Internet of Things (IoT) factories. Ultra-reliable low-latency communication (URLLC) effectively ensures real-time and reliable data transmission in factory environments [1]. However, the system's high-performance requirements significantly increase energy consumption, leading to operational costs and exacerbating environmental impact. Thus, in resource allocation, besides spectral efficiency (SE), energy efficiency (EE) must be fully considered to meet green communication requirements.

Nevertheless, maximizing SE requires higher transmission power, which in turn leads to a reduction in EE, thereby imposing a mutual constraint between the two [2], [3]. Moreover, communication scenarios and application requirements differ significantly across terminal types. Certain ground terminals (GTs) generate small data volumes and operate over extended periods, necessitating EE operation. In contrast, certain aerial terminals (ATs) prioritize high data throughput to support time-critical applications, thereby emphasizing SE [4]. The trade-off optimization between EE and SE is thus imperative.

Traditionally, the trade-off between EE and SE has been addressed using iterative optimization algorithms, such as swarm intelligence-based optimization algorithms (SIOAs) and Successive Convex Approximation (SCA) [6]. However, such algorithms generally have high complexity and face difficulties in convergence in complex application scenarios, making them unable to meet the strict real-time requirements of URLLC. In recent years, deep neural networks (DNNs) have been widely applied to resource allocation problems in CF-mMIMO systems [5], demonstrating efficient and stable performance advantages. DNN training typically adopts two approaches: supervised learning and unsupervised learning. The former requires a large amount of high-precision labeled data, leading to high data preparation costs [7]. In contrast, the latter optimizes the objective function by capturing the intrinsic feature structure of data, thus exhibiting higher flexibility. Nevertheless, due to the lack of guidance from labels, unsupervised models often have insufficient generalization capabilities [8].

Against this background, we propose an unsupervised EE-SE trade-off power allocation network (U-ESTPANet) for GTs and ATs in the CF-mMIMO uplink system of smart IoT factories. The main contributions are as follows:

- We design an unsupervised power allocation network (U-ESTPANet) to explicitly capture the distinct channel characteristics of GTs and ATs. This network employs dual-stream parallel inputs to independently extract spatial multipath features from GT and AT channels and operates without labeled data, significantly reducing training complexity compared to supervised learning approaches.
- We propose a weight-driven trade-off mechanism embedded within the unsupervised learning framework. By utilizing the weights to flexibly navigate the SE-EE trade-off relationship, the network determines a target operating point, thereby achieving a precise, customized balance between EE and SE that addresses the differentiated service requirements of GTs and ATs.
- Numerical simulations verify the proposed method's effectiveness, showing it achieves differential EE-SE trade-offs for GTs and ATs and outperforms traditional iterative algorithms in comprehensive and real-time performance.

(*Corresponding author: Donggen Li.*)

S. Yan, D. Li, W. Jiang and W. Feng are with the School of Microelectronics and Communication Engineering, Chongqing University, Chongqing 400044, China (email: yanshuaicheng@stu.cqu.edu.cn; lidonggen@stu.cqu.edu.cn; whjiang@cqu.edu; fengwj@cqu.edu.cn).

P. Xiao is with the 5GIC and 6GIC, Institute for Communication Systems, University of Surrey, GU2 7XH Guildford, U.K. (e-mail: p.xiao@surrey.ac.uk).

Kanapathippillai Cumanan and Alister Graham Burr are with the School of Physics, Engineering and Technology, University of York, YO10 5DD York, U.K. (e-mail: kanapathippillai.cumanan@york.ac.uk; alister.burr@york.ac.uk).

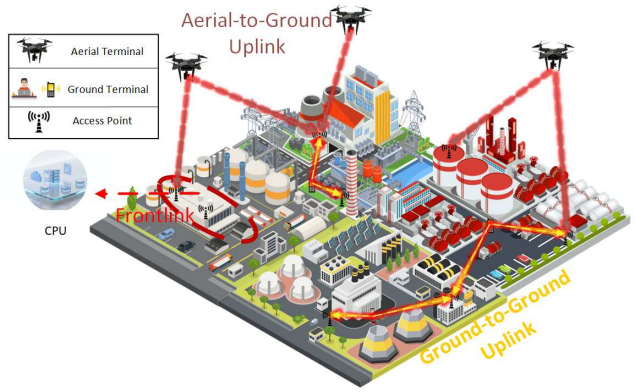

Fig. 1. Smart IoT factory CF-mMIMO system.

II. SYSTEM MODEL AND PROBLEM FORMULATION

Consider a CF-mMIMO uplink system in a smart IoT factory scenario, where M APs with L antennas collectively serve K terminals. These terminals include GTs and ATs, each subject to block fading channels caused by physical obstacles and electromagnetic interference common in industrial environments. All APs connect to a central processing unit (CPU) via error-free fronthaul links for joint signal processing. The system operates in the time-division duplex (TDD) mode with time-frequency resources partitioned into coherence blocks. Each terminal transmits a D-bit short data packet within N channel uses (CUs), where $N = BT_{\text{tm}}$, B is the system bandwidth [9], and T_{tm} is the transmission delay [10].

A. Uplink Signal Transmission

To satisfy the requirements of URLLC, pilot sequences $\boldsymbol{s}_{(\text{p}),k} \in \mathbb{C}^{1\times n_{(\text{p})}}$ and transmitted data $\boldsymbol{s}_{(\text{d}),k} \in \mathbb{C}^{1\times n_{(\text{d})}}$ with block length $n_{(\text{p})}$ and $n_{(\text{d})}$ are encapsulated into a short data packet for transmission. For the k-th AT, the channel to the m-th AP follows a Rician distribution, which is expressed as:

$$\mathbf{H}_{m,k} = \sqrt{\frac{\rho\beta_{m,k}}{\rho+1}}\boldsymbol{h}^{(\text{L})}_{m,k} + \sqrt{\frac{\beta_{m,k}}{\rho+1}}\boldsymbol{h}^{(\text{N})}_{m,k}. \tag{1}$$

However, for the k-th GT, due to the obstruction of complex terrain, the channel to the m-th AP degrades to a Rayleigh distribution [11], i.e., $\rho = 0$:

$$\mathbf{H}_{m,k} = \sqrt{\beta_{m,k}}\boldsymbol{h}^{(\text{N})}_{m,k}, \tag{2}$$

where ρ is the Rician factor, and $\beta_{m,k}$ denotes the large-scale fading coefficient, which includes the path loss and shadowing effect between the k-th terminal and the m-th AP. $\boldsymbol{h}^{(\text{L})}_{m,k} = [e^{j\theta_{m,k,1}}, \cdots, e^{j\theta_{m,k,L}}]^T \in \mathbb{C}^{L\times 1}$ is a random variable vector of LoS, $j = \sqrt{-1}$, and $\theta_{m,k,l}(l \in \{1, \cdots, L\})$ is a random variable uniformly distributed between $[-\pi, \pi]$. $\boldsymbol{h}^{(\text{N})}_{m,k} \in \mathbb{C}^{L\times 1}$ is a NLoS random variables following an independent and identically distributed (i.i.d.) $\mathcal{CN}(0,1)$, respectively.

Thus, the received signal at the m-th AP is expressed as:

$$\mathbf{Y}_m = \sum_{k=1}^{K}\sqrt{p_k}\mathbf{H}_{m,k}\left[\mathbf{S}_{(\text{p}),k}, \mathbf{S}_{(\text{d}),k}\right] + \left[\mathbf{N}_{(\text{p}),k}, \mathbf{N}_{(\text{d}),k}\right], \tag{3}$$

where p_k represents terminal transmission power, $\mathbf{N}_{(\text{p}),m} \in \mathbb{C}^{L\times n_{(\text{p})}}$ and $\mathbf{N}_{(\text{d}),k} \in \mathbb{C}^{L\times n_{(\text{d})}}$ denote the additive white Gaussian noise (AWGN) of pilot and data signals with independent and identically distributed (i.i.d.) $\mathcal{CN}(0,1)$, respectively.

To avoid the impact of pilot contamination, different terminals are assigned mutually orthogonal pilot signals with a specific blocklength, i.e., $\left\|\boldsymbol{s}_{(\text{p}),k}\right\|^2 = n_{(\text{p})}$, $\boldsymbol{s}_{(\text{p}),k}\boldsymbol{s}^{\text{H}}_{(\text{p}),\hat{k}} = 0 \quad (\hat{k} \neq k)$, and $\mathbb{E}(\left|\boldsymbol{s}_{(\text{p}),k}\right|^2) = 1$. The data signals $\boldsymbol{s}_{(\text{d}),k}$ are statistically uncorrelated with each other, i.e., $\mathbb{E}(|\boldsymbol{s}_{(\text{d}),k}|^2) = 1$ and $\mathbb{E}(s_{(\text{d}),k\hat{j}}s_{(\text{d}),kj}) = 0$ $(\hat{j} \neq j)$.

In the considered CF-mMIMO system, all APs estimate the approximate channel state via pilot signals. Herein, a low-complexity least squares (LS) method [12] is used for channel estimation, with the estimated channel coefficient between the m-th AP and k-th terminal denoted by

$$\begin{aligned}\hat{\mathbf{H}}_{m,k} &= \frac{1}{n_{(\text{p})}\sqrt{p_k}}\left(\sqrt{p_k}\mathbf{H}_{m,k}\mathbf{S}_{(\text{p}),k} + \mathbf{N}_{(\text{p}),k}\right)\left(\mathbf{S}_{(\text{p}),k}\right)^H \\ &= \mathbf{H}_{m,k} + \hat{\mathbf{W}}_{m,k},\end{aligned} \tag{4}$$

where $\hat{\mathbf{W}}_{m,k} = \frac{\mathbf{N}_{m,k}\left(\mathbf{S}_{(\text{p}),k}\right)^H}{n_{(\text{p})}\sqrt{p_k}} \in \mathbb{C}^{L\times 1}$ is the estimation error.

To accurately determine the data, a two-stage signal detection method is designed to suppress inter-user interference (IUI) caused by all users sharing spectrum resources. Specifically, the estimated channel $\hat{\mathbf{H}}_{m,k}$ is applied as a weight to the received signal of each AP, and then the normalized large-scale coefficient $\hat{\eta}_{m,k} = \frac{\beta_{m,k}}{\sum_{q=1}^{K}\beta_{m,q}}$ is used as an additional weight for the CPU. However, the CPU is unaware of the actual channel $\mathbf{H}_{m,k}$. The APs considered in this work are equipped with large-scale antenna arrays, leading to the channel hardening effect [13], that is, $\hat{\mathbf{H}}^H_{m,k}\hat{\mathbf{H}}_{m,k} \approx \mathbb{E}[\hat{\mathbf{H}}^H_{m,k}\mathbf{H}_{m,k}]$. The post-processing signal of the k-th terminal is expressed as:

$$\begin{aligned}\gamma_k = (DS_k)\mathbf{S}_{(\text{d}),k} &+ \sum_{\substack{i=1\\ i\neq k}}^{K}(IT_{ki})\mathbf{S}_{(\text{d}),i} \\ &- \sum_{i=1}^{K}(EW_{ki})\mathbf{S}_{(\text{d}),i} + AW_{ki},\end{aligned} \tag{5}$$

where $DS_k = \sum_{m=1}^{M}\sqrt{p_k}\hat{\eta}_{m,k}\hat{\mathbf{H}}^H_{m,k}\hat{\mathbf{H}}_{m,k}$ denotes the desired signal, $IT_{ki} = \sum_{m=1}^{M}\sqrt{p_k}\hat{\eta}_{m,i}\hat{\mathbf{H}}^H_{m,k}\hat{\mathbf{H}}_{m,i}$ denotes the IUI, $EW_{ki} = \sum_{m=1}^{M}\sqrt{p_k}\hat{\eta}_{m,k}\hat{\mathbf{H}}^H_{m,k}\hat{\mathbf{W}}_{m,i}$ denotes the estimation error, and $AW_{ki} = \sum_{m=1}^{M}\hat{\eta}_{m,k}\hat{\mathbf{H}}^H_{m,k}\hat{\mathbf{N}}_{m,k}$ denotes AWGN, respectively. For simplicity, define $EA_{ki} = \mathbb{E}\left|EW_{ki}\right|^2 + \mathbb{E}\left|AW_{ki}\right|^2$, then the signal-to-interference-plus-noise ratio (SINR) [9] of the k-th terminal is given by

$$\delta_k = \frac{\mathbb{E}\left\{\left|DS_k\right|^2\right\}}{\sum_{\substack{i=1\\ i\neq k}}^{K}\mathbb{E}\left\{\left|IT_{ki}\right|^2\right\} + \sum_{i=1}^{K}EA_{ki}}. \tag{6}$$

B. Performance Analysis

In this subsection, the closed expressions of reliability, delay, EE, and SE are formulated for the CF-mMIMO systems under URLLC constraints. Since the traditional Shannon formula capacity is insufficient to accurately characterize the achievable transmission rate under short data packet conditions, current research typically employs the finite blocklength (FBL) theory to characterize the short data packet transmission error probability (EP) [4]. Specifically, the EP of the k-th terminal is expressed as:

$$\epsilon_k = Q\left(\frac{\log_2(1+\delta_k) - R_k}{\sqrt{\frac{V(\delta_k)}{n_{(\mathrm{d})}}}}\right), \tag{7}$$

where $Q(c) = \frac{1}{\sqrt{2\pi}}\int_c^{\infty} e^{-t^2/2}dt$ is the probability that a random variable with independent and identically distributed $\mathcal{CN}(0,1)$ exceeds a constant value c, $V(\delta_k) = \left[1-(1+\delta_k)^{-2}\right]\log_2^2 e$ is the channel dispersion coefficient under the FBL regime, and R_k denotes the achievable data rate of the k-th terminal.

EE and SE are other key metrics not discussed in URLLC requirements but play a pivotal role in system performance. In the absence of power outage events, the system SE is expressed as the average of the achievable rates of all users (in bps/Hz), expressed as

$$SE = \frac{\sum_{k=1}^{K} R_k}{K}. \tag{8}$$

The system EE is defined as the ratio between the sum of SE and the total energy consumption, denoted by (in bits/J)

$$EE = \frac{B \times \sum_{k=1}^{K} R_k}{\sum_{k=1}^{K}(p_k\mu_k + \sigma_k)}, \tag{9}$$

where μ_k denotes the reciprocal of the power amplifier efficiency, and σ_k represents the static circuit power. The denominator reflects the total user-side power consumption, focusing on the energy expenditure of uplink terminals.

From Eqs. (7), (8) and (9), a trade-off relationship between EE and SE is demonstrated. To facilitate joint optimization, we propose a novel normalized metric:

$$\Omega = \Omega_{\mathrm{g}} + \Omega_{\mathrm{a}}, \tag{10}$$

where $\Omega_{\mathrm{g}} = (\lambda - \alpha_g)\widetilde{SE}_{\mathrm{g}} + \alpha_g\widetilde{EE}_{\mathrm{g}}$ and $\Omega_{\mathrm{a}} = \alpha_a\widetilde{SE}_{\mathrm{a}} + (\lambda-\alpha_a)\widetilde{EE}_{\mathrm{a}}$. α_g, α_a ($\in [0, 0.5]$) are the trade-off parameters, and distinct configurations assign customized trade-off targets to terminals. The proportional constant λ is set to 0.5. Based on the boundary values of EE and SE obtained from dataset statistics, the normalized SE and EE are defined as follows:

$$\widetilde{SE}_{\mathrm{g}} = \frac{SE_{\mathrm{g}} - SE_{\mathrm{g}}^{\min}}{SE_{\mathrm{g}}^{\max} - SE_{\mathrm{g}}^{\min}}, \quad \widetilde{EE}_{\mathrm{g}} = \frac{EE_{\mathrm{g}} - EE_{\mathrm{g}}^{\min}}{EE_{\mathrm{g}}^{\max} - EE_{\mathrm{g}}^{\min}}, \tag{11}$$

$\widetilde{SE}_{\mathrm{a}}$ and $\widetilde{EE}_{\mathrm{a}}$ follow the same principle. Finally, the optimization model is formulated as

$$\begin{aligned} \max_{p_k\ (k=1,2,\ldots,K)} \quad & \Omega, \\ \text{s.t.} \quad & p_{\min} \le p_k \le p_{\max}, \\ & t_E \le t_{\mathrm{QoS}}, \\ & \epsilon_k \le \epsilon_{\mathrm{QoS}}. \end{aligned} \tag{12}$$

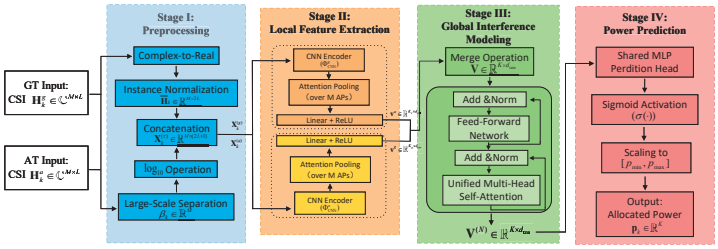

Fig. 2. The architecture of the proposed U-ESTPANet.

where $p_{\max}$ and $p_{\min}$ denote the maximum and minimum transmission powers, t_E is the end-to-end delay, t_{QoS} and ϵ_{QoS} represent the URLLC latency and EP constraints, respectively.

However, the fractional form of EE, defined as the ratio of SE to power, renders the optimization non-convex. This is further complicated by the nonlinear reliability constraint in Eqs. (7) under FBL theory. Consequently, such joint EE-SE problems are non-convex and intractable for traditional iterative algorithms [2], [5]. For this reason, we adopt a deep learning-based framework to achieve efficient solution.

III. Unsupervised Learning for Resource Optimization

To address the non-convexity of joint EE-SE optimization and high latency of iterative algorithms, we propose an unsupervised[1] power allocation network (U-ESTPANet). As shown in Fig. 2, the framework adopts a dual-stream differentiated perception architecture and comprises three core modules: Preprocessing Module, Independent Spatial Feature Extraction Module, and Global Interference Modeling Module.

Let $\mathcal{K}_g$ and $\mathcal{K}_a$ denote the sets of GTs and ATs, respectively. Given the significant divergence in their channel distributions, we construct two parallel preprocessing pipelines to generate independent input tensors $\mathbf{X}_k^{(g)}$ and $\mathbf{X}_k^{(a)}$.

For an arbitrary terminal k, the complex channel matrix is first converted to a real-valued matrix $\mathbf{H}_k^{real}$. To eliminate magnitude fluctuations caused by path loss and extract pure spatial multipath waveforms, Instance Normalization (IN) is applied:

$$\bar{\mathbf{H}}_k = \mathrm{InstanceNorm}(\mathbf{H}_k^{\mathrm{real}}). \quad \bar{\mathbf{H}}_k \in \mathbb{R}^{M\times 2L} \tag{13}$$

Subsequently, to explicitly preserve macroscopic geometric features critical for power allocation, we align the large-scale fading coefficient β_k via logarithmic mapping: $e_k = \log_{10}(\beta_k)$. Finally, these components are concatenated along the feature dimension to construct physically consistent inputs:

$$\mathbf{X}_k^{\tau} = [\bar{\mathbf{H}}_k^{\tau} \parallel e_k^{\tau}] \in \mathbb{R}^{M\times(2L+1)}, \quad \tau \in \{g, a\} \tag{14}$$

where $[\cdot \parallel \cdot]$ denotes the concatenation operation along the feature dimension, and τ identifies the terminal type.

To capture the distinct spatial features of GT and AT, two convolutional neural network mapping functions with independent parameters are designed: $\Phi_{\mathrm{CNN}}^{(g)}(\cdot)$ and $\Phi_{\mathrm{CNN}}^{(a)}(\cdot)$:

$$\mathbf{Z}_k^{\mathrm{conv}} = \Phi_{\mathrm{CNN}}^{\tau}(\mathbf{X}_k^{\tau}), \quad k \in \mathcal{K}_\tau \tag{15}$$

[1]Here, "unsupervised" means training without explicit labels by directly optimizing the formulated loss.

where $\mathbf{Z}_k^{\text{conv}} \in \mathbb{R}^{d_{\text{cnn}} \times M}$ denotes the intermediate feature map, and d_{cnn} is set to 128. Subsequently, an Attention Pooling layer is employed to aggregate features along the AP dimension, which suppresses noise interference from invalid APs and generates the compact embedding vector $v_k \in \mathbb{R}^{d_{\text{cnn}}}$:

$$v_k = \text{AttnPool}(\mathbf{Z}_k^{\text{conv}}). \tag{16}$$

To capture global interference, terminal features are aggregated into $\mathbf{V} \in \mathbb{R}^{K \times d_{\text{cnn}}}$ and processed by a 2-layer Transformer. The attention matrix at layer l is computed as:

$$\mathbf{A}^{(l)} = \text{softmax}\left(\frac{\mathbf{Q}^{(l)}(\mathbf{K}^{(l)})^T}{\sqrt{d_{\text{cnn}}}}\right), \tag{17}$$

where $\mathbf{Q}^{(l)} = \mathbf{V}^{(l-1)}\mathbf{W}_Q$ and $\mathbf{K}^{(l)} = \mathbf{V}^{(l-1)}\mathbf{W}_K$. This mechanism captures the interference topology and yields the context-aware features $\mathbf{V}^{(N)} \in \mathbb{R}^{K \times d_{\text{cnn}}}$.

Finally, $\mathbf{V}^{(N)}$ is fed into a shared MLP to predict normalized power coefficients. A sigmoid activation is applied to strictly satisfy power constraints $[p_{\min}, p_{\max}]$:

$$\mathbf{p} = p_{\min} + (p_{\max} - p_{\min}) \cdot \sigma(\text{MLP}(\mathbf{V}^{(N)})), \tag{18}$$

where $\sigma(\cdot)$ denotes the Sigmoid activation function, and the MLP consists of a single affine transformation layer.

Accounting for the differential optimization requirements of GTs and ATs, the loss function is formulated as [5]:

$$loss = \gamma_1 loss_1 + \gamma_2 loss_2, \tag{19}$$

where $loss_1 = \text{avg}(\epsilon_k - \epsilon_{\text{QoS}})$ ($k \in K$ and $\epsilon_k > \epsilon_{\text{QoS}}$) and $loss_2 = \frac{1}{1+\Omega}$ are designed to ensure that all terminal devices satisfy the URLLC reliability requirements. γ_1 and γ_2 denote the weights of the respective loss components, which are empirically set to 5 and 1 in this work.

IV. SIMULATIONS AND RESULTS

A. Simulation Parameter Setting

In this section, the performance of the proposed algorithm is simulated, with specific simulation parameters listed in Table I [14]. In particular, a CF-mMIMO uplink system with a side length of 1000 meters is considered. In this scenario, a total of M uniformly distributed APs are deployed to serve K randomly distributed terminals, where the ratio of GTs to ATs is maintained at 1:1. Referring to [15], the large-scale fading coefficient between the k-th terminal and the m-th AP is modeled as:

$$\beta_{k,m} = -30.5 - 37.6 \log_{10}(d_{k,m}) + \Psi, \tag{20}$$

where $d_{i,j}$ denotes the distance (in meters) between the i-th user equipment and the j-th access point, and Ψ is the shadow fading coefficient with a standard deviation of 8.

B. Analysis of Experimental Results

This subsection evaluates U-ESTPANet against maximum power and CVX-solved SCA baselines, focusing on the EE-SE trade-off for GTs and ATs under strict URLLC constraints.

In terms of network configuration, we set the batch size to 8, the initial learning rate to 0.001, and the training duration to 200 epochs, utilizing the Adam optimizer for acceleration. Regarding the dataset, 1500 sets of large-scale coefficients are generated according to Eq. (20) and divided into training and testing sets with a 9:1 ratio. The simulations are conducted on a computing platform equipped with an Intel i7 processor (2.10 GHz), 8 GB RAM, and a GTX 2060 GPU, using PyCharm 2023.2.1. Additionally, for the sake of intuitive visualization, we uniformly set α_g and α_a as α in this analysis.

Figs. 3 and 4 show the comparison results of SE and EE for GTs and ATs under different quantities, where the trade-off parameter α = 0.25 (representing the maximum trade-off between SE and EE). As the number of terminals K increases, the interference between devices gradually intensifies, leading

Table I. Simulation Parameters

Parameters	Value
Carrier frequency (GHz)	1.9
Bandwidth (MHz)	10
Frame length of data (bits)	32
Frame length of pilot (bits)	64
Delay constrain of URLLC (ms)	0.5
Blocklength of data (CUs)	2000
Error probability constraint of URLLC	10^{-5}
Number of antennas per AP	16
Number of APs	64
The ratio of ATs to GTs	1:1
Maximum transmission power (W)	1
Minimum transmission power (W)	0.001

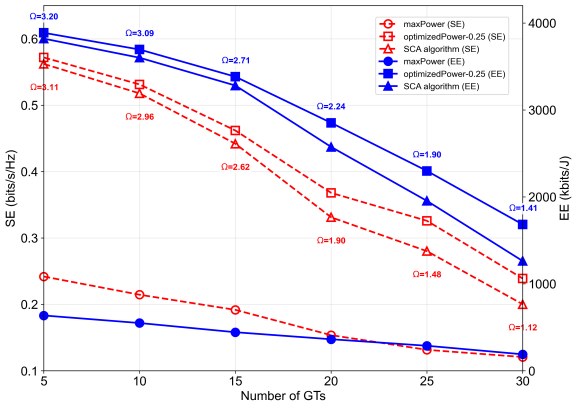

Fig. 3. Comparison of SE and EE across the number of GTs.

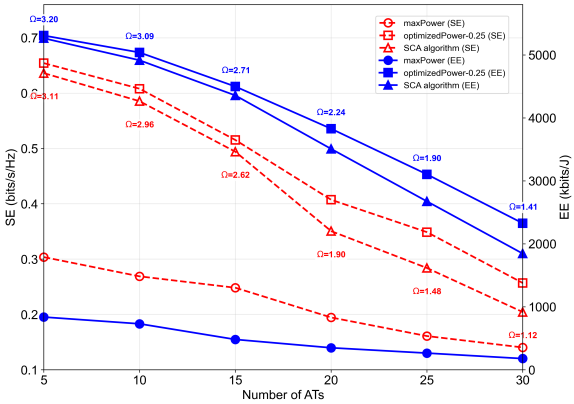

Fig. 4. Comparison of SE and EE across the number of ATs.

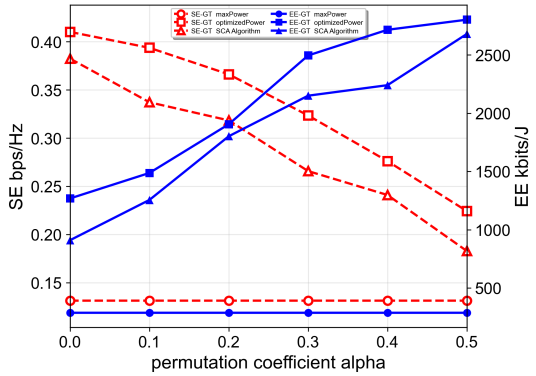

Fig. 5. Comparison of SE and EE across α in GTs.

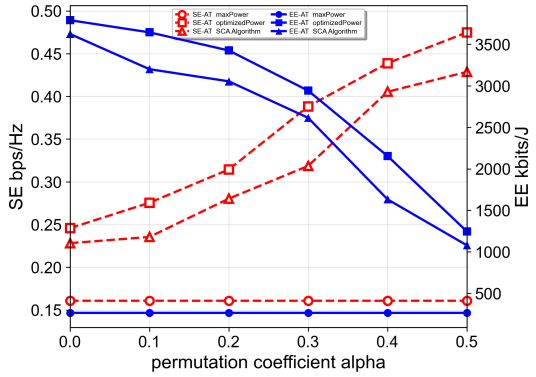

Fig. 6. Comparison of SE and EE across α in ATs.

to a decrease in SINR and data rate. Consequently, both EE and SE of all power allocation schemes show a downward trend with the increase of K, thereby reducing the optimization objective Ω.

Relative to the $p_{\max}$ benchmark, U-ESTPANet improves both the EE and SE for GTs and ATs by effectively maximizing the optimization objective Ω, though performance gains diminish as the system scales. Regarding computational overhead, the SCA algorithm, with a per-iteration complexity of $O(K^3)$, incurs prohibitive latencies of 4.23 s at $K = 10$ and 14.21 s at $K = 60$ after 20 iterations, failing to satisfy strict URLLC requirements. In contrast, the proposed unsupervised model executes a single forward inference with $O(KML + lK^2 d_{\text{cnn}})$ complexity without requiring label generation. It achieves a stable average runtime of 0.36 ms, providing a reliable solution for URLLC systems in IoT factories.

Figs. 5 and 6 illustrate performance variations against α for $K = 50$ devices. At this scale, the traditional SCA algorithm fails to fully converge, yielding oscillating and inferior results. In contrast, U-ESTPANet remains stable and enables flexible resource reconfiguration: a higher setting ($\alpha = 0.4$) prioritizes energy efficiency for GTs (EE $\approx$ 2715 kbits/J), whereas a lower setting ($\alpha = 0.1$) maximizes throughput for ATs (SE $\approx$ 0.44 bps/Hz). This verifies U-ESTPANet's superiority in convergence stability and differentiated EE-SE trade-offs.

V. CONCLUSION

We propose U-ESTPANet, an unsupervised deep learning framework optimizing the EE-SE trade-off in URLLC CF-mMIMO uplinks. By tailoring power allocation to diverse terminal requirements, it overcomes the limited adaptability of traditional iterative algorithms. It enhances real-time performance and eliminates labeled data preparation costs. Simulations confirm it substantially optimizes EE and SE while maintaining stability.

By learning channel state-to-power mappings, U-ESTPANet generalizes to other URLLC scenarios (e.g., smart grids) and adapts to various constraints by adjusting objective functions. This efficient solution highlights the broad prospects of unsupervised learning in next-generation networks.

REFERENCES

[1] J. Xue, K. Yu, T. Zhang, H. Zhou, L. Zhao, and X. Shen, "Cooperative deep reinforcement learning enabled power allocation for packet duplication URLLC in multi-connectivity vehicular networks," *IEEE Trans. Mobile Comput.*, vol. 23, no. 8, pp. 8143–8157, 2024.

[2] R. Allu, M. Katwe, K. Singh, S. L. Cotton, C.-P. Li, and T. Q. Duong, "Robust beamforming design for RSMA-integrated full-duplex communications: Energy and spectral efficiency trade-off," *IEEE Trans. Green Commun. Netw.*, vol. 9, no. 3, pp. 948–961, 2025, doi: 10.1109/TGCN.2024.3466295.

[3] Y. Yang, S. Dang, M. Wen, and M. Guizani, "Millimeter wave MIMO-OFDM with index modulation: A Pareto paradigm on spectral-energy efficiency trade-off," *IEEE Trans. Wireless Commun.*, vol. 20, no. 10, pp. 6371–6386, 2021.

[4] M. Li, Y. Huang, F. R. Yu, P. Si, and H. Zhang, "Ambient backscatter communication-assisted intelligent resource management for green industrial IoT," *IEEE Wireless Commun.*, vol. 32, no. 1, pp. 174–181, 2025, doi: 10.1109/MWC.001.2400040.

[5] D. Li, J. Li, D. Niyato, W. Feng, and W. Jiang, "Deep energy-efficient optimization network for URLLC over cell-free massive MIMO," *IEEE Internet Things J.*, vol. 12, no. 12, pp. 20973–20987, 2025, doi: 10.1109/JIOT.2025.3547933.

[6] G. Scutari, F. Facchinei, P. Song, D. P. Palomar, and J.-S. Pang, "Decomposition by partial linearization: Parallel optimization of multi-agent systems," *IEEE Trans. Signal Process.*, vol. 62, no. 3, pp. 641–656, 2014.

[7] R. Zhang, K. Xiong, Y. Lu, D. W. K. Ng, P. Fan, and K. B. Letaief, "SWIPT-enabled cell-free massive MIMO-NOMA networks: A machine learning-based approach," *IEEE Trans. Wireless Commun.*, vol. 23, no. 7, pp. 6701–6718, 2024.

[8] Y. Zhang, J. Zhang, S. Buzzi, H. Xiao, and B. Ai, "Unsupervised deep learning for power control of cell-free massive MIMO systems," *IEEE Trans. Veh. Technol.*, vol. 72, no. 7, pp. 9585–9590, 2023.

[9] J. Zeng, T. Wu, Y. Song, Y. Zhong, T. Lv, and S. Zhou, "Achieving energy-efficient massive URLLC over cell-free massive MIMO," *IEEE Internet Things J.*, vol. 11, no. 2, pp. 2198–2210, 2024.

[10] D. Galappaththige and C. Tellambura, "Sum rate maximization for RSMA-assisted CF mMIMO networks with SWIPT users," *IEEE Wireless Commun. Lett.*, vol. 13, no. 5, pp. 1300–1304, 2024.

[11] C. Huang, X. Chen, G. Chen, P. Xiao, G. Y. Li, and W. Huang, "Deep reinforcement learning-based resource allocation for hybrid bit and generative semantic communications in space-air-ground integrated networks," *IEEE J. Sel. Areas Commun.*, early access, 2025, doi: 10.1109/JSAC.2025.3623157.

[12] W. Yang, M. Li, and Q. Liu, "A practical channel estimation strategy for XL-MIMO communication systems," *IEEE Commun. Lett.*, vol. 27, no. 6, pp. 1580–1583, 2023.

[13] A. M. Tulino and S. Verdú, "Random matrix theory and wireless communications," *Found. Trends Commun. Inf. Theory*, vol. 1, no. 1, pp. 1–182, 2004.

[14] Y. Lu *et al.*, "Energy-efficient RIS-aided cell-free massive MIMO systems: Application, opportunities, and challenges," *IEEE Wireless Commun.*, vol. 32, no. 4, pp. 148–155, 2025, doi: 10.1109/MWC.001.2400224.

[15] E. Björnson and L. Sanguinetti, "Making cell-free massive MIMO competitive with MMSE processing and centralized implementation," *IEEE Trans. Wireless Commun.*, vol. 19, no. 1, pp. 77–90, 2020.